

## Schiff base ligand and metal (II) complex: Synthesis, characterization and biological evaluation

Dipen Panchani, Tirth Thaker\* & Chaitali Lamse

Department of Chemistry, Parul Institute of Applied Sciences, Parul University, Waghodiya, Vadodara 391 760, Gujarat, India

E-mail: tirth6582@gmail.com

Received 7 November 2024; accepted (revised) 22 January 2025

Mixed ligand complexes of Cu (II), Ni (II), Mg (II), Hg (II) and Fe (II) with an innovative Schiff base ligand denoted as (L1), (Z)-2-(1-hydrazineylideneethyl)-3H-benzo[f]chromen-3-one and (L2), (E)-2-(1-(2-phenylhydrazineylidene)ethyl)-3H-benzo[f]chromen-3-one, as the principal ligands have been synthesized and characterized. Assessments include elemental analyses and mass spectrometry, Fourier transform-infrared and ultraviolet-visible spectroscopy. The mixed ligand complex has been evaluated for its antibacterial activity against two Gram-positive bacteria (*Bacillus subtilis*, MTCC 441 and *Staphylococcus aureus*, MTCC 96) and two Gram-negative bacteria (*Pseudomonas aeruginosa*, MTCC 1866 and *Escherichia coli*, MTCC 443).

**Keywords:** Schiff base complex, Spectral studies, Anti-microbial activity

One of the significant groups of ligands that has garnered attention and is growing quickly is known as the Schiff base. This is because of its industrial, thermal, and biological uses<sup>1</sup>. It is commonly known that the interaction of metal ions with Schiff bases yields flexible binding sites, which result in materials with intriguing features like the ability to bind oxygen reversibly, catalytic conversion reactions (such as the hydrogenation of olefins), amino group transfer, photochromic, optical, magnetic, and sensing characteristics. Schiff bases' transition metal complexes, made from amines and aldehydes, have been studied extensively<sup>2,3</sup>.

The Schiff base contains donor atoms of nitrogen and oxygen, which facilitate easy coordination with transition metal ions to produce increased thermally stable and colorful metal complexes<sup>4</sup>. In coordination chemistry, using organic ligands containing heteroatoms as coordination sites has been a significant approach that has produced a wide range of fascinating and useful compounds. The strong chelating capacity of ligands with multiple donor heteroatoms has attracted interest worldwide because it allows for the development of mono-, di-, or multinuclear complexes<sup>5,6</sup>.

In biological processes, metal ions are crucial. Medicinal inorganic chemistry is the branch of study that focuses on using inorganic chemistry to treat or diagnose illnesses. One of the primary subfields of bioinorganic chemistry is the introduction of metal

ions or metal ion binding components into a biological system to treat illnesses. Intentionally injecting metal ions into the human body has shown promise in therapeutic and diagnostic applications<sup>7</sup>. In medicinal chemistry, organic-metal complexes are crucial for detecting and treating various illnesses, including cancer, arthritis, and antimicrobial, antifungal, and antiparasitic drugs<sup>8</sup>.

Researcher interest in solid-state thermal kinetic investigations of transition metal complexes including nitrogen and oxygen donor ligands has been growing due to scientific advancement and the rapid development of technology<sup>9</sup>. Activation energy, pre-exponential factor, and reaction order were among the thermal behavior of Schiff-base metal complexes that were extensively studied using a variety of analysis techniques<sup>10</sup>. These compounds go through decomposition reactions upon thermal treatment, releasing heat, gaseous products, and solid metal oxide residues that can be utilized in the creation of environmental sensors for the detection of various hazardous materials at trace levels, as well as in explosives, propellants, and pyrotechnic compounds<sup>11</sup>.

Due to the many applications that result from their selectivity, sensitivity, stability, and simplicity of synthesis, among other qualities, Schiff bases are among the classes of chemical compounds most studied by scientists<sup>12</sup>. Amidst their well-studied bioactive medicinal and pharmacological uses,

azomethines, as they are sometimes known, have found usage as catalysts, analytical reagents, and azo compounds for use as pigments and dyes, either in their original form or by modifications. They also demonstrated mild steel corrosion inhibition properties in  $\text{H}_2\text{SO}_4$  experiments conducted at various concentrations and temperatures<sup>13,14</sup>.

The objective of this research is to synthesize a Schiff base ligand ( $\text{L}_1$ ) via the condensation process of 2-acetyl-3*H*-benzo[*f*]chromen-3-one with Hydrazine hydrate and Phenyl hydrazine and subsequently develop its corresponding complexes with metal (Fig. 1). A thorough analysis using a variety of physicochemical approaches was used for characterization. The study also looks at the Schiff base's biological properties and related metal complexes, including its antibacterial properties.

## Experimental Section

### Materials and Methods

All chemicals were purchased from commercial sources (LOBA chem, Spectrochem, Merck, and Sigma-Aldrich). Melting points were determined using the equipronics model EQ-730 instrument and are uncorrected. TLC was carried out using Merck silica gel 60 F254 plates. Visualization of the plates was done using a UV lamp ( $\lambda_{\text{max}} = 254$  or 365 nm).  $^1\text{H}$  NMR spectra were recorded using Bruker 400MHz NMR spectrometer in  $\text{DMSO-}d_6$  solution and TMS as internal standard. IR spectra were recorded using the Bruker alpha FTIR spectrometer. Mass spectral data were recorded using a Shimadzu LC2010 mass analyser and C, H, N analysis using Perkin Elmer PE 2400.

### Synthesis of 2-acetyl-3*H*-benzo[*f*]chromen-3-one, 1

A mixture of 2-hydroxy-1-naphthaldehyde (0.01 mol), ethyl acetoacetate (0.01 mol), and pyridine (10 mL) in a 50 mL round-bottom flask, the addition of 2-3 drops piperidine (catalytic amount) to the reaction

mixture was left overnight in the bulb. After completion, the reaction solution was poured into ice:HCl (90:10), crude product was filtered, dried, and recrystallized from ethanol as yellow crystals. Yield 81%. m.p.185.3°C. IR (KBr): 1733 (C=O), 1671 (C=O) 1553 (C=C), 1238 (C-O), 973  $\text{cm}^{-1}$  (C-H);  $^1\text{H}$  NMR ( $\text{DMSO-}d_6$ , 400 MHz):  $\delta$  2.66 (s, 3H, -COCH<sub>3</sub>), 7.61 (m, 1H), 7.68 (m, 1H), 7.78 (dd, 1H), 8.08 (d, 1H), 8.32 (d, 1H), 8.61 (dd, 1H), 9.27 (s, 1H); ESI-MS:  $m/z$  239.11  $\text{C}_{15}\text{H}_{10}\text{O}_3$  requires 238.24. Anal. Calcd for C, 75.62; H, 4.23. Found: C, 75.78; H, 4.12%.

### Synthesis of Schiff bases ligand [ $\text{L}_1/\text{L}_2$ ]

2-Acetyl-3*H*-benzo[*f*]chromen-3-one (1 mol) and hydrazine hydrate/phenyl hydrazine (1 mol) were dissolved in ethanol (10 mL), 2-3 drops of sulfuric acid were added in a 50 mL round-bottom flask was refluxed for 4-6 h. After completion of the reaction, the solid product obtained was collected, filtered, washed with 100 mL water, dried, and then crystallized from ethanol. Spectral data are analysed as under  $\text{L}_1/\text{L}_2$

**(Z)-2-(1-Hydrazineylideneethyl)-3*H*-benzo(F) chromen-3-one [Ligand  $\text{L}_1$ ]:** Yield 75%. m.p.257.3°C. IR (KBr): 3200-3500 (N-H), 1710 (C=O), 1596 (C=N), 1508 (N-H), 1215 (C-N), 1056 (C-O), 810  $\text{cm}^{-1}$  (C-H);  $^1\text{H}$  NMR ( $\text{DMSO-}d_6$ , 400 MHz):  $\delta$  2.08 (s, 3H, -CH<sub>3</sub>), 7.02 (s, 2H, -NH<sub>2</sub>), 7.32 (m, 2H), 7.51 (dd, 1H), 7.76 (dd, 1H), 7.93 (d, 1H), 8.03 (s, 1H, -NH) 8.87 (s, 1H); ESI-MS:  $m/z$  253.44  $\text{C}_{15}\text{H}_{12}\text{N}_2\text{O}_2$  requires 252.27. Anal. Calcd for C, 71.42; H, 4.79; N, 11.10. Found: C, 71.83; H, 4.66; N, 11.33%.

**(E)-2-(1-(2-Phenylhydrazineylidene) ethyl)-3*H*-benzo[*f*]chromen-3-one [Ligand  $\text{L}_2$ ]:** Yield 61%. m.p.199.2°C. IR (KBr): 3372 (N-H), 1700 (C=O), 1630 (C=N), 1502 (N-H), 1214 (C-N), 1056 (C-O), 810  $\text{cm}^{-1}$  (C-H);  $^1\text{H}$  NMR ( $\text{DMSO-}d_6$ , 400 MHz):

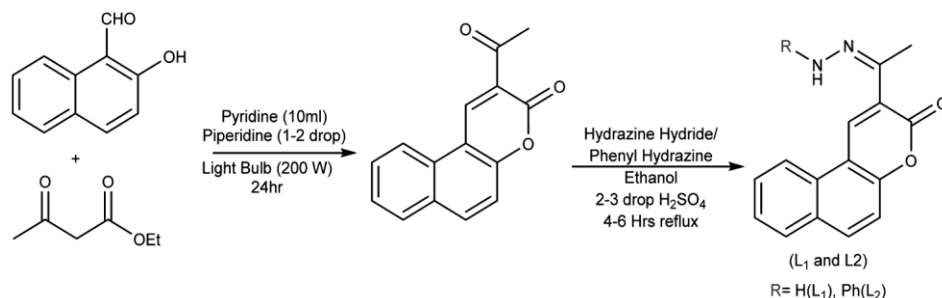


Fig. 1 — Synthetic route for Schiff base ligand ( $\text{L}_1$  and  $\text{L}_2$ )

$\delta$  2.66 (s, 3H, -CH<sub>3</sub>), 6.99 (m, 1H), 7.17 (m, 2H), 7.36 (dd, 2H), 7.46 (d, 1H), 7.52 (d, 1H), 7.55 (m, 1H), 7.65 (s, 1H), 7.66 (m, 1H), 8.09 (dd, 1H), 8.46 (dd, 1H), 8.92 (s, 1H, -NH); ESI-MS:  $m/z$  328.37 C<sub>21</sub>H<sub>16</sub>N<sub>2</sub>O<sub>2</sub> requires 326.22. Anal. Calcd for C, 76.81; H, 4.91; N, 8.53. Found: C, 76.63; H, 4.34; N, 8.83%.

### Synthesis of Metal Complexes

Ligand L<sub>1</sub> or L<sub>2</sub> (2 mol) were soluble in 20 mL EtOH and metal salt (1 mol) is also dissolved in the pure EtOH mixed in 50 mL RBF and refluxed at 80°C for 6-7 h. After the reaction was completed, the separated complex mixture was filtered using a Buchner funnel and washed with cold ethanol to dry it (Fig. 2).

### Synthesis of metal complexes with (Z)-2-(1-hydrazineylideneethyl)-3H-benzo(F)chromen-3-one and (E)-2-(1-(2-phenylhydrazineylidene) ethyl)-3H-benzo[f]chromen-3-one [Ligand L<sub>1</sub>/L<sub>2</sub>]

**CuL<sub>1</sub>**: Yield 68%. m.p.290.0°C. IR (KBr): 1619 (C=C), 1577 (N-H), 1462 (-CH<sub>3</sub>), 1311 (C-N), 1278 (C-O), 1080 cm<sup>-1</sup> (C-H); MS:  $m/z$  598.12 C<sub>30</sub>H<sub>26</sub>CuN<sub>6</sub>O<sub>4</sub> requires 597.13. Anal. Calcd for C, 60.24; H, 4.38; Cu, 10.62; N, 14.05. Found: C, 60.88; H, 4.24; Cu, 10.61; N, 14.98%.

**NiL<sub>1</sub>**: Yield 77%. m.p.308.4°C. IR (KBr): 1619 (C=C), 1573 (N-H), 1460 (-CH<sub>3</sub>), 1311 (C-N), 1278 (C-O), 1080 cm<sup>-1</sup> (C-H); MS:  $m/z$  594.14 C<sub>30</sub>H<sub>26</sub>N<sub>6</sub>NiO<sub>4</sub> requires 593.27. Anal. Calcd for C, 60.74; H, 4.42; N, 14.17; Ni, 9.89. Found: C, 60.74; H, 4.42; N, 14.17; Ni, 9.89%.

**HgL<sub>1</sub>**: Yield 75%. m.p.310.2°C. IR (KBr): 1738 (C=O), 1619 (C=C), 1578 (N-H), 1466 (-CH<sub>3</sub>), 1319 (C-N), 1280 (C-O), 1027 cm<sup>-1</sup> (C-H); MS:  $m/z$  736.17; C<sub>30</sub>H<sub>26</sub>HgN<sub>6</sub>O<sub>4</sub> requires 735.17. Anal. Calcd

for: C, 49.01; H, 3.56; Hg, 27.28; N, 11.43. Found: C, 49.87; H, 3.20; Hg, 27.52; N, 11.16%.

**MgL<sub>1</sub>**: Yield 68%. m.p.260.6°C. IR (KBr): 3221 (O=H), 1620 (C=C), 1461 (-CH<sub>3</sub>), 1310 (C-N), 1234 (C-O), 1074 cm<sup>-1</sup> (C-H); MS:  $m/z$  559.19 C<sub>30</sub>H<sub>26</sub>MgN<sub>6</sub>O<sub>4</sub> requires 558.88. Anal. Calcd for: C, 64.47; H, 4.69; Mg, 4.35; N, 15.04. Found: C, 64.92; H, 4.12; Mg, 4.38; N, 15.87%.

**FeL<sub>1</sub>**: Yield 82%. m.p.265.3°C. IR (KBr): 3496 (N-H), 3392 (O-H), 2923 (C-H), 1619 (C=N), 833 (H<sub>2</sub>O), 629 (M-N), 486 cm<sup>-1</sup> (M-O); MS:  $m/z$  591.42 C<sub>30</sub>H<sub>26</sub>FeN<sub>6</sub>O<sub>4</sub> requires 590.48. Anal. Calcd for: C, 61.03; H, 4.44; Fe, 9.46; N, 14.23. Found: C, 61.67; H, 4.32; Fe, 9.73; N, 14.10%.

**CuL<sub>2</sub>**: Yield 77%. m.p.180.9°C. IR (KBr): 1619 (C=C), 1577 (N-H), 1462 (-CH<sub>3</sub>), 1311 (C-N), 1278 (C-O), 1080 cm<sup>-1</sup> (C-H); MS:  $m/z$  721.17 C<sub>42</sub>H<sub>32</sub>CuN<sub>4</sub>O<sub>4</sub> requires 720.29. Anal. Calcd for C, 70.04; H, 4.48; Cu, 8.82; N, 7.78. Found: C, 70.16; H, 4.34; Cu, 8.38; N, 7.96%.

**NiL<sub>2</sub>**: Yield 69%. m.p.240.2°C. IR (KBr): 1619 (C=C), 1573 (N-H), 1460 (-CH<sub>3</sub>), 1311 (C-N), 1278 (C-O), 1080 cm<sup>-1</sup> (C-H); MS:  $m/z$  716.18 C<sub>42</sub>H<sub>32</sub>N<sub>4</sub>NiO<sub>4</sub> requires 715.44. Anal. Calcd for: C, 70.51; H, 4.51; Ni, 8.20. Found: C, 70.91; H, 4.29; N, 7.45; Ni, 8.64%.

**HgL<sub>2</sub>**: Yield 74%. m.p.220.0°C; IR (KBr): 1738 (C=O), 1619 (C=C), 1578 (N-H), 1466 (-CH<sub>3</sub>), 1319 (C-N), 1280 (C-O), 1027 cm<sup>-1</sup> (C-H); MS:  $m/z$  859.80 C<sub>42</sub>H<sub>32</sub>HgN<sub>4</sub>O<sub>4</sub> requires 858.21. Anal. Calcd for C, 58.84; H, 3.76; Hg, 23.40; N, 6.54. Found: C, 58.17; H, 3.06; Hg, 23.67; N, 6.88%.

**MgL<sub>2</sub>**: Yield 85%. m.p.250.1°C. IR (KBr): 3221 (O=H), 1620 (C=C), 1461 (-CH<sub>3</sub>), 1310 (C-N), 1234 (C-O), 1074 cm<sup>-1</sup> (C-H); MS:  $m/z$  682.23

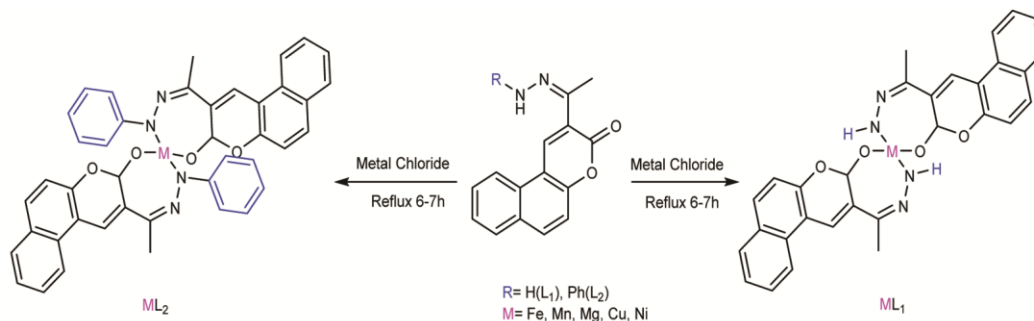


Fig. 2 — Structure of the mixed ligands complexes and their formation reaction

$C_{42}H_{32}MgN_4O_4$  requires 681.05. Anal. Calcd for C, 74.07; H, 4.74; Mg, 3.57; N, 8.23. Found: C, 74.99; H, 4.12; Mg, 3.55; N, 8.49%.

**FeL<sub>2</sub>**: Yield 71%. m.p.260.8°C. IR (KBr): 1577 (N-H), 1462 (-CH<sub>3</sub>), 1311 (C-N), 1279 (C-O), 1081 cm<sup>-1</sup> (C-H); MS: *m/z* 713.43  $C_{42}H_{32}FeN_4O_4$  requires 712.59. Anal. Calcd for C, 70.79; H, 4.53; Fe, 7.84; N, 7.86. Found: C, 70.05; H, 4.32; Fe, 7.67; N, 7.43%.

## Results and Discussion

### Chemistry

In the present investigation, synthesis of the target compound is shown as 3 step reaction, where starting compound 2-acetyl-3*H*-benzo[*f*]chromen-3-one **1** was synthesized by condensation of 2-hydroxy naphthaldehyde and ethyl acetoacetate in pyridine and catalytic amount piperidine left for 24 h under 100 W bulb. The crude product was purified by recrystallization in ethanol and a pale-yellow solid was obtained with 71% yield. It was confirmed through IR and <sup>1</sup>H NMR spectra. The IR spectrum of **1** showed C=O (Ester) at 1733 cm<sup>-1</sup>, C=O (Ketone) at 1671 cm<sup>-1</sup>, aromatic ring breathing vibration C=C at 1553 cm<sup>-1</sup>, O-H at 1340 cm<sup>-1</sup> and C-O at 1238 cm<sup>-1</sup>. <sup>1</sup>H NMR of compound **1** indicated COCH<sub>3</sub> at δ 2.66 as a singlet and aromatic proton were observed between 7.61 at δ 9.27. Compound **1** was treated with hydrazine hydrate/phenyl hydrazine dissolved in ethanol and refluxed in the presence of H<sub>2</sub>SO<sub>4</sub> for 4-6 hrs to obtain (L<sub>1</sub> Schiff base of hydrazine hydrate/L<sub>2</sub> Schiff base of phenyl hydrazine) L<sub>1</sub> as yellow and L<sub>2</sub> as maroon solid with 75 and 61% yield. IR spectrum of L<sub>1</sub> showed C=O at 1710 cm<sup>-1</sup>, N=O at 1596 cm<sup>-1</sup>,

O-H bend at 1393 cm<sup>-1</sup>, and C-H bend at 1056 cm<sup>-1</sup>. <sup>1</sup>H NMR of **2a** indicated peak confirmative signals of -COCH<sub>3</sub> at 2.5 and -NH proton at δ 8.3 and aromatic protons at δ 8.15-6.50. The IR spectrum of compound **2b** showed C=C stretch at 1599 cm<sup>-1</sup>, C-H bend at 951 cm<sup>-1</sup>, and O-H bend at 1319 cm<sup>-1</sup>. <sup>1</sup>H NMR of **1** indicated peak confirmative signals of -COCH<sub>3</sub> at δ 3.7, -NH proton at δ 9.3 and aromatic protons at δ 7.6-8.1. The analytical and physical data of the Schiff base and its metal complexes are shown in Table 1.

### FT-IR

The FT-IR spectral data containing relevant characteristic band regions of the ligand and its metal complexes are jotted down in Table 2. The Metal complex formation has been confirmed by the Disappearance of C=O ketone group band at 1700-1710 cm<sup>-1</sup> and the presence of a ν(N-H) band at 1561-1578 cm<sup>-1</sup> indicates that the Schiff-base condensation occurred between hydrazine hydrate and phenylhydrazine.

### UV-Vis absorption spectra

The spectral parameters calculated by the Tanabe-Sugano diagram, band positions of absorption maxima, band assignments, and proposed geometry are listed in Table 3 (Ref. 2). The hyperchromic shift in metal complex spectra confirmed the coordination of ligands toward metal ions. Synthesis of 2-acetyl-3*H*-benzo [*f*]chromen-3-one shows UV-Vis absorption at 255.0 nm wavelength. Whereas the Schiff base ligands obtained (E)-2-(1-(2-phenylhydrazineylidene) ethyl)-3*H*-benzo[*f*]chromen-3-one (L<sub>2</sub>) shows UV-Vis absorption at 319.0 nm wavelength and (Z)-2-(1-hydrazineylideneethyl)-3*H*-

Table 1 — Analytical and physical data of the Schiff base and its metal complexes

| Compd                  | Mol. Wt. | Colour        | State | m.p. (°C) | Yield (%) | Found (%) |      |       |
|------------------------|----------|---------------|-------|-----------|-----------|-----------|------|-------|
|                        |          |               |       |           |           | C         | H    | N     |
| <b>1</b>               | 238.24   | Golden yellow | Solid | 175.3     | 88        | 75.78     | 4.12 | —     |
| <b>L<sub>1</sub></b>   | 252.27   | Light yellow  | Solid | 257.3     | 85        | 71.83     | 4.66 | 11.33 |
| <b>L<sub>2</sub></b>   | 328.37   | Orange        | Solid | 199.2     | 76        | 76.63     | 4.32 | 8.83  |
| <b>CuL<sub>1</sub></b> | 598.12   | Light brown   | Solid | 290.0     | 68        | 60.88     | 4.24 | 14.98 |
| <b>NiL<sub>1</sub></b> | 592.14   | Yellow        | Solid | 308.4     | 77        | 60.74     | 4.42 | 14.17 |
| <b>HgL<sub>1</sub></b> | 736.17   | Lemon yellow  | Solid | 310.2     | 75        | 49.87     | 3.20 | 11.16 |
| <b>MgL<sub>1</sub></b> | 558.19   | Orange        | Solid | 260.6     | 68        | 64.92     | 4.12 | 15.87 |
| <b>FeL<sub>1</sub></b> | 590.42   | Light orange  | Solid | 265.3     | 82        | 61.67     | 4.32 | 14.10 |
| <b>CuL<sub>2</sub></b> | 719.17   | Lemon yellow  | Solid | 180.9     | 77        | 70.16     | 4.34 | 7.96  |
| <b>NiL<sub>2</sub></b> | 714.18   | Dark yellow   | Solid | 240.2     | 69        | 70.91     | 4.29 | 8.64  |
| <b>HgL<sub>2</sub></b> | 272.80   | Yellow        | Solid | 220.0     | 74        | 58.17     | 3.06 | 6.88  |
| <b>MgL<sub>2</sub></b> | 680.23   | Yellow        | Solid | 250.1     | 85        | 74.99     | 4.12 | 8.49  |
| <b>FeL<sub>2</sub></b> | 712.18   | Brown         | Solid | 260.8     | 71        | 70.05     | 4.32 | 70.43 |

Table 2 — Infrared spectral data of the ligand and its complexes

| Compd                  | $\nu \text{ cm}^{-1}$ (CH <sub>3</sub> ) | $\nu \text{ cm}^{-1}$ (C=C) | $\nu \text{ cm}^{-1}$ (C=O) | $\nu \text{ cm}^{-1}$ (C-N) | $\nu \text{ cm}^{-1}$ (N-H) |
|------------------------|--|-----------------------------|-----------------------------|-----------------------------|-----------------------------|
| <b>1</b>               | 1460                                     | 1553                        | 1733, 1671                  | —                           | —                           |
| <b>L<sub>1</sub></b>   | 1453                                     | —                           | 1710                        | 1215                        | 1508                        |
| <b>L<sub>2</sub></b>   | 1465                                     | —                           | 1700                        | 1214                        | 1502                        |
| <b>CuL<sub>1</sub></b> | 1462                                     | 1619                        | —                           | 1311                        | 1577                        |
| <b>NiL<sub>1</sub></b> | 1460                                     | 1619                        | —                           | 1311                        | 1573                        |
| <b>HgL<sub>1</sub></b> | 1466                                     | 1619                        | —                           | 1319                        | 1578                        |
| <b>MgL<sub>1</sub></b> | 1461                                     | 1620                        | —                           | 1310                        | 1570                        |
| <b>FeL<sub>1</sub></b> | 1462                                     | 1619                        | —                           | 1311                        | 1577                        |
| <b>CuL<sub>2</sub></b> | 1462                                     | 1619                        | —                           | 1311                        | 1577                        |
| <b>NiL<sub>2</sub></b> | 1460                                     | 1619                        | —                           | 1311                        | 1573                        |
| <b>HgL<sub>2</sub></b> | 1466                                     | 1619                        | —                           | 1319                        | 1578                        |
| <b>MgL<sub>2</sub></b> | 1461                                     | 1620                        | —                           | 1310                        | 1561                        |
| <b>FeL<sub>2</sub></b> | 1462                                     | 1620                        | —                           | 1311                        | 1577                        |

Table 3 — UV-Vis  $\lambda$  max value of the synthesized Schiff bases and their metal complexes

| Compd                  | Wavelength (UV-Vis $\lambda$ max) |
|------------------------|-----------------------------------|
| <b>1</b>               | 255.0                             |
| <b>L<sub>1</sub></b>   | 255.0                             |
| <b>L<sub>2</sub></b>   | 319.0                             |
| <b>CuL<sub>1</sub></b> | 383.0                             |
| <b>NiL<sub>1</sub></b> | 420.0                             |
| <b>HgL<sub>1</sub></b> | 384.0                             |
| <b>MgL<sub>1</sub></b> | 256.0                             |
| <b>FeL<sub>1</sub></b> | 262.0                             |
| <b>CuL<sub>2</sub></b> | 290.0                             |
| <b>NiL<sub>2</sub></b> | 444.0                             |
| <b>HgL<sub>2</sub></b> | 261.0                             |
| <b>MgL<sub>2</sub></b> | 271.0                             |
| <b>FeL<sub>2</sub></b> | 248.0                             |

benzo(F)chromen-3-one (L1) UV-Vis absorption at 255.0 nm wavelength. Whereas complexes of L<sub>1</sub> show CuL<sub>1</sub> and HgL<sub>1</sub>, UV-Vis absorption at 383.0 nm wavelength. Similarly, MgL<sub>1</sub> and FeL<sub>1</sub> showed UV-Vis absorption at 256-262 nm wavelength. Only NiL<sub>1</sub> showed higher absorption of 420nm wavelength in this L<sub>1</sub> series. For the L<sub>2</sub> series of metal complexes CuL<sub>2</sub>, HgL<sub>2</sub>, MgL<sub>2</sub>, and FeL<sub>2</sub> showed UV-Vis absorption at 240-290 nm wavelength and NiL<sub>2</sub> appeared at 444.0 nm wavelength (Fig. 3).

## Biological activity

### Antibacterial activity

Using the diffusion plate method, synthesized compounds were evaluated for antibacterial activity. A 9 cm diameter plate filled with solid bacterial medium was inoculated with a specified amount (25  $\mu$ L) of the sample (5 mM) using a HiMedia blank disc. The material exhibited encouraging inhibitory power against bacterial strains during the 24-hour incubation period at 37°C, as indicated by the

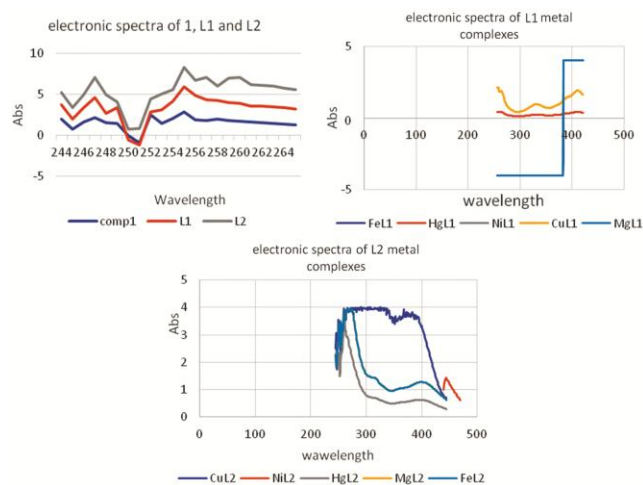


Fig. 3 — UV-Vis graph of ligand and metal complex

measurement of the zone of inhibition's diameter. Two Gram-positive bacteria (*Bacillus subtilis*, MTCC 441, and *Staphylococcus aureus*, MTCC 96) and two Gram-negative bacteria (*Pseudomonas aeruginosa*, MTCC 1866, and *Escherichia coli*, MTCC 443) were used to test the antibacterial activity of the chemical in toxicity (Table 4).

### ADME Studies

Studies using the absorption, distribution, metabolism, and excretion (ADME) method were conducted to the ADME of these substances. It evaluates the bloodstream's drug-likeness using a computer method. Specific techniques can be used to analyze each of these processes separately. The physicochemical properties of Lipinski, Ghose, Veber, Egan, Muegge, and the compound's bioavailability score, for instance, provide information on drug-likeness. The Brain or Intestinal Estimated Permeation, which is based on Egan's multi-statistical

Table 4 — Antimicrobial activity of the synthesized compound and standard

| Compd                  | Antibacterial Activity                        |                |                            |                  |
|------------------------|---|----------------|----------------------------|------------------|
|                        | Microorganisms and zone of inhibition (mm/mg) |                |                            |                  |
|                        | Gm <sup>-ve</sup> bacteria                    |                | Gm <sup>+ve</sup> bacteria |                  |
|                        | <i>P. aeruginosa</i>                          | <i>E. coli</i> | <i>B. subtilis</i>         | <i>S. aureus</i> |
| <b>1</b>               | 9   | 11             | 8                          | 12               |
| <b>L<sub>1</sub></b>   | 9   | 12             | 10                         | 12               |
| <b>L<sub>2</sub></b>   | 12  | 13             | 8                          | 9                |
| <b>FeL<sub>1</sub></b> | 10  | 11             | 10                         | 15               |
| <b>HgL<sub>1</sub></b> | 10  | 12             | 13                         | 12               |
| <b>NiL<sub>1</sub></b> | 8   | 9              | 13                         | 13               |
| <b>CuL<sub>1</sub></b> | 12  | 11             | 11                         | 10               |
| <b>MgL<sub>1</sub></b> | 9   | 11             | 12                         | 8                |
| <b>FeL<sub>2</sub></b> | 8   | 13             | 8                          | 13               |
| <b>HgL<sub>2</sub></b> | 10  | 9              | 13                         | 10               |
| <b>NiL<sub>2</sub></b> | 11  | 11             | 6                          | 11               |
| <b>CuL<sub>2</sub></b> | 10  | 11             | 11                         | 12               |
| <b>MgL<sub>2</sub></b> | 8   | 12             | 10                         | 10               |
| Penicillin-G           | 23  | 18             | 14                         | 14               |

Table 5 — Druglikeness, pharmacokinetics, medicinal chemistry properties and ADME studies of synthesized derivatives

| Compd                  | Lipinski drug like |       |     |     | Veber drug like |    | Solubility         | Absorption and distribution |      |     |     |
|------------------------|--------------------|-------|-----|-----|-----------------|----|--------------------|-----------------------------|------|-----|-----|
|                        | Mol. wt.           | MlogP | HBA | HBD | TPSA            | RB | ESOL               | WlogP                       | GI   | Pgp | BBB |
| <b>1</b>               | 238.24             | 2.17  | 3   | 0   | 47.28           | 1  | Soluble            | 3.15                        | High | No  | Yes |
| <b>L<sub>1</sub></b>   | 252.27             | 2.13  | 3   | 1   | 68.59           | 1  | Soluble            | 2.63                        | High | No  | Yes |
| <b>L<sub>2</sub></b>   | 328.36             | 3.6   | 3   | 1   | 54.6            | 3  | Moderately soluble | 4.59                        | High | No  | Yes |
| <b>CuL<sub>1</sub></b> | 594.12             | 3.42  | 7   | 2   | 110.93          | 0  | Poorly soluble     | 4                           | High | Yes | No  |
| <b>NiL<sub>1</sub></b> | 589.27             | 3.42  | 7   | 2   | 110.93          | 0  | Poorly soluble     | 4.01                        | High | Yes | No  |
| <b>HgL<sub>1</sub></b> | 731.17             | 3.42  | 7   | 2   | 110.93          | 0  | Poorly soluble     | 4                           | High | Yes | No  |
| <b>MgL<sub>1</sub></b> | 554.88             | 3.42  | 7   | 2   | 110.93          | 0  | Poorly soluble     | 4.01                        | High | Yes | No  |
| <b>FeL<sub>1</sub></b> | 586.42             | 3.42  | 7   | 2   | 110.93          | 0  | Poorly soluble     | 4                           | High | Yes | No  |
| <b>CuL<sub>2</sub></b> | 720.27             | 4.94  | 6   | 0   | 68.12           | 2  | Insoluble          | 7.56                        | Low  | Yes | No  |
| <b>NiL<sub>2</sub></b> | 715.42             | 4.94  | 6   | 0   | 68.12           | 2  | Insoluble          | 7.56                        | Low  | Yes | No  |
| <b>HgL<sub>2</sub></b> | 857.32             | 4.94  | 6   | 0   | 68.12           | 2  | Insoluble          | 7.56                        | Low  | Yes | No  |
| <b>MgL<sub>2</sub></b> | 681.03             | 4.94  | 6   | 0   | 68.12           | 2  | Insoluble          | 7.56                        | Low  | Yes | No  |
| <b>FeL<sub>2</sub></b> | 712.57             | 4.94  | 6   | 0   | 68.12           | 2  | Insoluble          | 7.56                        | Low  | Yes | No  |

Note: Mol. wt. - Molecular weight, MlogP- Topological method implemented, HBA- H-Bond Acceptor, HBD- H-Bond Donors, TPSA- Topological polar surface area, RB- Rotatable bonds ESOL- Estimated aqueous solubility, WlogP- atomistic method implemented, GI- Gastrointestinal absorption, P-gp- P-glycoprotein substrate, BBB- Blood-brain barrier parameter.

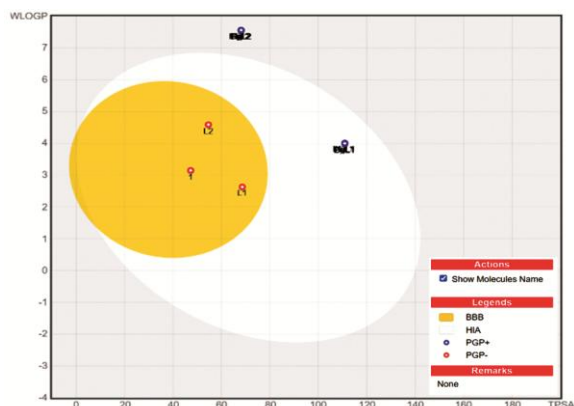


Fig. 4 — BOILED-Egg representation of Schiff bases and their metal complexes

graph model 44, forecasts CNS access and human intestinal absorption (HIA) through a breach in the blood-brain barrier by using polarity (TPSA) and lipophilicity (WlogP). A linear trend is thus followed by the ellipse formed by the intersection of the polarity and lipophilicity profiles (Table 5, Fig. 4), which accounts for both highly and poorly absorbed compounds in the human intestine.

## Conclusion

In conclusion, the present work reports the synthesis, characterization, and biological activity of a series of metal complexes of Schiff base ligands (Z)-2-(1-hydrazineylideneethyl)-3H-benzo(F)chromen-3-

one and (E)-2-(1-(2-phenylhydrazineylidene) ethyl)-3H-benzo[f]chromen-3-one. The starting material used to prepare Schiff bases 2-acetyl-3H-benzo[f]chromen-3-one (1) was synthesized using 2-hydroxy-1-naphthaldehyde and ethyl acetoacetate. The synthesized compounds show excellent activity against all micro-organisms. The ADME studies on these complexes showed that the activity of a drug on the body of the synthesized metal complexes revealed good biological potential of Cu(II), Co(II), Mn(II), Ni(II), and Mg(II) complexes of hydrazine hydride showed remarkably active against gastrointestinal penetration of the drug. In contrast, the metal complexes of phenyl hydrazine are toxic. The synthesized compounds may be used as a lead compound discovery for new antimicrobial agents.

### References

- 1 Warad I, Ali O, Ali AA, Jaradat NA, Hussein F, Abdallah L, Al-Zaqri N, Alsalmeh A & Alharthi F A, *Molecules*, 25 (2020) 2253.
- 2 Buldurun K, Turan N, Bursal E, Mantarçı A, Turkan F, Taslimi P & Gulcin I, *Res Chem Intermed*, 46 (2020) 283.
- 3 Ahmad N, Alam M, Wahab R, Ahmed M & Ahmad A, *Open Chem*, (2020). (<https://doi.org/10.1515/chem-2020-0168>).
- 4 Joshi N R, Mule S G, Gore V A., Suryawanshi R D, Pawar G T, Bembalkar S R & Pawar R P, *J Exp Res Pharm*, 7 (2022) 202.
- 5 Mohapatra R K, Sarangi A K, Mohammad A, El-Ajaily M M, Kudrat-E-Zahan M, Patjoshi S B & Dash Dhruva C, *J Mol Struct*, 1179 (2019) 65.
- 6 Mansour M S A, Abdelkarim A T, El-Sherif A A & Mahmoud W H, *BMC Chem*, 18 (2024) 150.
- 7 Fahmy H M, Abdel-Rahman F M., El-Sayed A A & El-Sherif A A, *BMC Chem*, 17 (2023) 78.
- 8 Nawaz M, Abbasi M W, Tariq Marium, Graham J P, Al-Hagri A-R S, Elkarim A A, Mohamed M E, Nissapatorn V, Taha M & Hisaindee S, *BMC Chem*, 16 (2022) 21.
- 9 Deschamps E., Ciminelli V. & Holl W, *Water Res*, 39 (2005) 5212.
- 10 Yang C, Ju T, Wang X, Ji Y, Yang C, Lv H, Wang Y, Dong W, Dang F, Shi X, Wang W & Fan Y, *RCS Adv*, 10 (2020) 10612.
- 11 Nugent J, Shire B R, Caputo D F J, Pickford H D, Nightingale F, Houlsby I T T, Mousseau J J & Anderson E A, *Ange Chemie Int Ed*, 59 (2020) 11866.
- 12 Akl M A., El-Mahdy N A., Elbadrawy Z, El-Zeny A S & Mostafa M M, *BMC Chem*, 17 (2023) 153.
- 13 Idemudia O G., Sadimenko A P & Hosten E C, *Int J Mol Sci*, 17 (2016) 687.
- 14 Abdel-Aziz H A, Mekawey A A I & Dawood K M, 44 (2009) 3637.